Received: 6 February 2019 | Revised: 26 June 2019 | Accepted: 8 August 2019

DOI: 10.1002/aic.16758

REACTION ENGINEERING, KINETICS AND CATALYSIS

AIChE JOURNAL

The solution of continuous kinetic lumping models using the adaptive characterization method

Daniele C. Rocha[1,2] | Paulo L. C. Lage[1]

[1]Programa de Engenharia Química—COPPE, Universidade Federal do Rio de Janeiro, Rio de Janeiro, RJ, Brazil

[2]PETROBRAS—Edifício Senado (EDISEN), Rio de Janeiro, RJ, Brazil

Correspondence
Paulo L. C. Lage, Programa de Engenharia Química—COPPE, Universidade Federal do Rio de Janeiro, PO Box 68502, 21941-972, Rio de Janeiro, RJ, Brazil.
Email: paulo@peq.coppe.ufrj.br

Funding information
Conselho Nacional de Desenvolvimento Científico e Tecnológico, Grant/Award Numbers: 305265/2015-6, 456905/2014-6; Coordenação de Aperfeiçoamento de Pessoal de Nível Superior, Grant/Award Number: Finance Code 001; Fundação Carlos Chagas Filho de Amparo à Pesquisa do Estado do Rio de Janeiro, Grant/Award Number: E-26/111.361/2010

Abstract

The continuous kinetic lumping models are traditionally solved by methods that discretize the mixture into a large number of pseudo-components. This works proposes the usage of the adaptive characterization of continuous mixtures, grounded on the direct quadrature method of generalized moments, in the solution of kinetic lumping models, which allows a large reduction in the number of pseudo-components. Catalytic hydrogenation and hydrocracking problems were used to evaluate this methodology, comparing its results with analytical solutions or results from a classical numerical method. The results showed that the proposed methodology could accurately solve those continuous kinetic models using a small number of adaptive pseudo-components, leading to a large reduction in the computational cost of simulation when compared to the classical numerical method.

KEYWORDS

adaptive characterization, continuous mixture, kinetic model, modeling and simulation, quadrature-based moment methods

1 | INTRODUCTION

Processes in several industries (oil and gas, petrochemical, biotechnology, pharmaceutical, etc.) have streams that are formed by continuous reactive mixtures. The design, analysis, and optimization of such processes may be carried by mathematical models that intend to describe the physical and chemical phenomena as close as possible to reality.

The so-called continuous reactive mixtures are multicomponent fluids composed by hundreds of species undergoing reactions. Since they have similar properties, it is not practical, or even possible, to identify all of them and their composition using customary quantitative analysis.[1]

In academic and scientific community, the modeling of continuous reactive mixtures have been a recurrent subject, since it is not yet fully understood and there is not a general consensus on the best way to approach it. Therefore, the subject of this work is relevant to both academic and industrial researches.

The thermodynamic and kinetic modeling of these mixtures often starts from the application of an order reduction method. These methods consist of characterizing a group of components through a single compound, preserving some of the group physical properties and its behavior in the relevant process.

Okino and Mavrovouniotis[2] reviewed the order reduction methods, classifying them into three types: sensitivity analysis, time-scale analysis and lumping. This work focused on the lumping strategy, more specifically on the continuous lumping approach. Further details regarding the other approaches can be found in Okino and Mavrovouniotis.[2]

The continuous approach has been used for a long time for modeling the thermodynamic and kinetic behavior of multicomponent mixtures. Regarding the kinetic modeling, the next section describes how this approach has evolved from a mathematical model often used for the fragmentation of particulate systems.

This model is a special case of the population balance equation (PBE), for pure particle breakage problems.[3] The PBE is an integro-differential equation that does not usually have an analytical solution. Thus, suitable numerical methods are essential for its solution.

The quadrature-based moment methods (QBMM; quadrature method of moments [QMoM], direct quadrature method of moments [DQMoM], direct quadrature method of generalized moments [DQMoGeM], etc.)

were originally proposed to solve PBEs, being used, extended and improved for this purpose in the past few years.[4-8]

Additionally, Lage[1] proposed an innovative application for the quadrature methods of moments: the solution of continuous thermodynamic problems. His work pointed out a remarkable characteristic of these methods: the ability of adapting the mixture characterization during the solution. Due to this, these adaptive methods are able to achieve accurate solutions with a small number of quadrature points, being more efficient than the fixed-abscissa quadrature rules or any other method based on a fixed discretization.

Following Lage[1] approach, Laurent et al.[9,10] applied QMoM to model the multicomponent droplet vaporization process. Later on, Rodrigues et al.[11] provided an adaptive scheme for the multistage separation of continuous multicomponent mixtures and, according to Petitfrere et al.,[12] the adaptive feature of QMoM has proven to be highly accurate for multiphase flash calculations.

The direct form of QMoM was also extended to field problems by Jatobá et al.,[13] widening its scope for continuous mixture characterization. However, there is no previous work, to the authors' knowledge, that applied QMoM or one of its variants to solve kinetic models of continuous mixtures, even though these models have evolved from the population balance formulation.

Therefore, this work developed an alternate methodology to solve kinetic models of continuous mixtures by using the adaptive QBMM method called DQMoGeM.[14] Three test cases were solved to verify its accuracy. It performance was compared to that of the numerical method of Laxminarasimhan et al.,[15] which is often used to solve hydrocracking reactions.

2 | MODELS FOR REACTIVE CONTINUOUS MIXTURES

2.1 | Kinetic modeling based on continuous lumping

DeDonder[16] was the first researcher to consider a multicomponent mixture as a continuous one, discussing the theory of reactions of continuous mixtures.[17-20]

While previous works addressed specific reactions, Aris and Gavalas[21] were the first to show how to model any first-order reaction (reversible or irreversible, isothermal or non-isothermal) using the continuous approach.

Considering the mixture distribution over a single conveniently chosen variable I, the molar concentration of the entire mixture, $C(t)$, is obtained from:

$$C(t) = \int_{I_{min}}^{I_{max}} f_C(I,t)dI \tag{1}$$

where f_C is the distribution of the molar concentration of the mixture.

For parallel independent first-order reactions, the individual reaction rates are given by:

$$\frac{\partial f_C(I,t)}{\partial t} = -k(I)f_C(I,t) \tag{2}$$

Ho and Aris[22] initiated the discussion regarding the effect of nonlinear kinetics of individual reactions on the kinetic modeling of continuous mixtures. They showed that the simple and straightforward extension of the continuous modeling used for linear reactions, Equation (2), to nonlinear reaction models causes inconsistencies due to the fact that f_C is a distribution and not a concentration.

Three different approaches were proposed to represent nonlinear kinetic models for the concentration distribution of a continuous mixture: cooperative nonlinear kinetics,[23] double-distributed continuous mixture[24] and coordinate transformation.[25]

This work focused on the coordinate transformation method, which proposed the introduction of the distribution function for the number of components, $D(I)$, whose definition implies that $D(I)dI$ gives the differential number of mixture components in the $[I, I + dI]$ interval. The idea behind this approach is to decompose the concentration distribution into two parts: the distribution $D(I)$ and the concentration of an individual component, $c(I)$, that is, $f_C(I) = D(I)c(I, t)$. Thus, the usual nonlinear kinetic models can be easily extended to continuous mixtures. For instance, a q-order decomposition reaction can be written as:

$$\frac{\partial c(I,t)}{\partial t} = -k(I)[c(I,t)]^q \tag{3}$$

which has the same form used for the reaction order of a single chemical species. This approach was applied in a widely used model for hydrocracking problems, described in the next section.

2.2 | Kinetic lumping modeling as a population balance model

The cracking reactions of a continuous mixture can be modeled using a special case of the PBE, which considers the evolution of a univariate distribution due to a fragmentation process in a spatially homogeneous problem, as shown by[3]:

$$\frac{\partial f(I,t)}{\partial t} = -b_f(I,t)f(I,t) + \int_I^\infty \nu(I')b_f(I',t)\Omega(I,I')f(I',t)dI' \tag{4}$$

where f is the particle number distribution function, b_f is the breakage frequency, ν is the average number of particles formed from the breakup of a single particle of state I' ($\nu = 2$ for binary fragmentation) and Ω is the probability distribution function for the daughter particles generated by the breakup of one particle of state I' have state I.

In Equation (4), $f(I, t)dI$ means the number of particles per unit of volume with label between I and $I + dI$. Thus, the total number of particles per unit of volume, $pn(t)$, is given by:

$$pn(t) = \int_{I_{min}}^{I_{max}} f(I,t)dI \tag{5}$$

According to Ramkrishna,[3] the same notions applied for particles are also valid for molecules, cells or other entities. Thus, the number density of particles in the kinetic context is actually the number

density of molecules, which gives the molar concentration when divided by the Avogadro number (N_{Av}): $C(t) = pn(t)/N_{Av}$. Therefore, Equations (1) and (5) are equivalent with $f_C = f/N_{Av}$.

In the context of continuous reactions, Saito[26] was the first to use the fragmentation model, Equation (4), to describe a polymer degradation process[27,28] in the following form:

$$\frac{\partial f_C(l,t)}{\partial t} = -\kappa(l) f_C(l,t) + 2\int_l^{l_{max}} k(l,l') f_C(l',t) dl' \tag{6}$$

where binary fragmentation was considered, the breakage frequency, b_f, was made equal to the overall rate function, κ, and $k(l, l')$ was interpreted as a stoichiometry coefficient, defined by:

$$k(l,l') = \kappa(l')\Omega(l,l') \tag{7}$$

Being a probability distribution with $\Omega(l, l') = 0$, $l > l'$, it is clear that

$$\int_0^l \Omega(l,l') dl = 1 \tag{8}$$

leading to

$$\kappa(l) = \int_0^l k(l,l') dl \tag{9}$$

However, the classic breakage formulation is intrinsically for first-order kinetics.[15,29] For this reason, Laxminarasimhan et al.[15] used the coordinate transformation approach[25] to propose a new model for hydrocracking that can consider nonlinear reactions with general stoichiometry. Their formulation was proposed in terms of the mass distribution, w, using the reactivity, k, as the distribution variable, as follows:

$$\frac{dw(k,t)}{dt} = -kw(k,t) + \int_k^{k_{max}} p(k,k') k' w(k',t) D(k') dk' \tag{10}$$

where $p(k, k')$ is the yield distribution function, that accounts for the formation of the component with reactivity k from the cracking of the component with reactivity k'. Laxminarasimhan et al.[15] pointed out that the usage of the distributions $D(k')$ and $p(k, k')$ make their formulation general enough to consider the cracking of any complex mixture. It should be noted that this model applies equally for the normalized or non-normalized mass distributions. In the former w is the mass fraction distribution and in the latter it is just the mass distribution. Laxminarasimhan et al.[15] analyzed the experimental data for the cracking of hydrocarbon families reported in the literature and proposed a skewed Gaussian function to model the yield distribution $p(k, k')$, using three adjustable parameters (a_0, a_1 and ψ).

Laxminarasimhan et al.[15] assumed that the reactivity is a function of the normalized true boiling point temperature, θ, which is often experimentally available for petroleum, using the following expression:

$$\theta = \frac{TBP - TBP_{min}}{TBP_{max} - TBP_{min}} = \left[\frac{k}{k_{max}}\right]^{\alpha} \tag{11}$$

where k_{max} is the highest reactivity in the mixture and α is a dimensionless parameter. Since the number of components in any arbitrary interval must be the same for any distribution variable, then:

$$D(k)dk = D(\theta)d\theta \tag{12}$$

and the number of lumps is given by:

$$n = \int_0^1 D(\theta) d\theta \tag{13}$$

Assuming an uniform $D(\theta)$ distribution, one can derive:

$$D(k) = \frac{n\alpha}{k_{max}^{\alpha}} k^{\alpha-1} \tag{14}$$

Thus, the Laxminarasimhan et al.[15] model has five adjustable parameters: α, k_{max}, a_0, a_1, and ψ. There are several works that reported good results by using the model proposed by Laxminarasimhan et al.[15] or its extensions.[30-38]

3 | THE NUMERICAL SOLUTION OF CONTINUOUS KINETIC MODELS

The governing equation for reacting continuous mixtures often has an integro-differential form, for example, Equation (10), which does not usually have an analytical solution. Two main numerical methodologies has been used to solve these models: the method of moments (MoM)[39] and a methodology proposed by Laxminarasimhan et al.[15] that combines a fixed discretization and a Gaussian quadrature, which is called here the fixed point quadrature method (FPQM).

The FPQM has been developed and mainly employed for hydrocarbon cracking. It basically consists in a characterization of $w(k, t)$ using n lumps and the time integration of the discretized form of the kinetic equation, Equation (10). The application of the FPQM to solve continuous kinetic lumping models was given in detail by Elizalde and Ancheyta.[34]

In this work, we proposed the application of the adaptive characterization method[1] to solve continuous kinetic reaction models for the first time. This method uses a QBMM to choose the pseudo-components. Here, we employed the DQMoGeM, which is a generalization of the direct version of the QMoM,[4] which in turn is a modification of the original MoM.[39]

The QMoM was the first QBMM developed and successfully applied to solve a wide range of population balance problems, due its ability of overcome the known closure problem of the MoM by approximating the integrals using the Gauss–Christoffel quadrature rule,[40] defined by:

$$\int_{l_{min}}^{l_{max}} g(l)f(l)dl \cong \sum_{i=1}^{N} \omega_i g(l_i) \tag{15}$$

where g is any function and f is the weight function, which is the distribution itself.

Lage[1] was the first to propose its usage to solve continuous thermodynamic problems as each quadrature point can be identified as a discretized pseudo-component. Besides, Equation (15) is the optimal quadrature for calculating the properties of a mixture with a molar fraction distribution given by $f(l)$.

However, the moment inversion problem in the QMoM is time-consuming and its general solution for multivariate distributions is not known. Thus, Marchisio and Fox[5] developed the direct version of QMoM (DQMoM) to eliminate the need for solving the moment inversion problem during the time evolution of f.

Its basic idea is to track explicitly the weights and the abscissas of the quadrature instead of the moments of the distribution. In order to achieve that, the DQMoM replaces the distribution by its discrete approximation, given by the following summation of N Dirac delta functions:

$$f(l,t) = \sum_{i=1}^{N} \omega_i(t)\delta(l - l_i(t)) \tag{16}$$

which gives the Gauss–Christoffel quadrature approximation represented by Equation (15) using the filtering property of the Dirac delta function:

$$\int_{l_{min}}^{l_{max}} g(l)\delta(l - l_i)dl = g(l_i), \quad \forall l_i \in (l_{min}, l_{max}) \tag{17}$$

The replacement of the distribution by Equation (16) in the moments of the PBE results in a system of differential equations for the weights and abscissas. Thus, the DQMoM requires the moment inversion procedure only once to find the initial condition.

The DQMoGeM is a generalization of the DQMoM in which the regular moments are substituted by the generalized moments, which are defined by:

$$\mu_j = \int_{l_{min}}^{l_{max}} P_j(l)f(l)dl, \quad j = 0, \ldots, 2N-1 \tag{18}$$

where P_j, j = 0, …, ∞, are the j-order members of a family of orthogonal polynomials in the same interval (l_{min}, l_{max}) in respect to a weight function $\mathcal{W}$, which satisfy the orthogonality property:

$$\int_{l_{min}}^{l_{max}} P_i(l)P_j(l)\mathcal{W}(l)dl = 0, \quad \forall i \neq j \tag{19}$$

Using the Gauss–Christoffel quadrature, the generalized moments can be written as:

$$\mu_j = \sum_{i=1}^{N} \omega_i P_j(l_i) \tag{20}$$

In the DQMoGeM, the moment operators are given by:

$$\int_{l_{min}}^{l_{max}} P_j(l)\cdot dl, \quad j = 0, \ldots, \infty, \tag{21}$$

whose application to the PBE generates the system of differential equations for the quadrature abscissas and weights.

The moments can be calculated from their definition using the weights and abscissas of the quadrature rule (Equation 20), being usually the only unknown variables that have to be determined. Sometimes, though, it is necessary to reconstruct the distribution from its moments.

Grosch et al.[6] were the first to reformulate the QMoM and DQMoM by using generalized moments. They used only Laguerre polynomials in semi-infinite domain problems, concluding that the methods were only marginally more robust than the corresponding methods using regular moments. On the other hand, Santos et al.[14] analyzed problems in semi-infinite and finite domains, using Laguerre and Legendre polynomials, respectively. They concluding that, for finite domain problems, the usage of Legendre polynomial moments improves the method robustness. The reformulated DQMoM was named as DQMoGeM by Santos et al.[14]

4 | APPLICATION OF THE DQMOGEM

The application of the DQMoGeM can be summarized in the following sequential steps:

1. For a known initial distribution function, calculate the initial moments, from Equation (18), and solve the moment inversion problem to determine the initial values for the weights and abscissas.
2. Derive the system of differential equations for the weights and abscissas by substituting the distribution function in the kinetic model by its discretization (Equation 16), applying the generalized moment operators (Equation 21) and the filtering properties of the Dirac delta distributions:

$$\int_{l_{min}}^{l_{max}} P_j(l)\delta^{(k)}(l - l_i)dl = (-1)^k P_j^{(k)}(l_i), \quad k = 0, 1, \ldots \tag{22}$$

3. Perform the time integration of the system of differential equations obtained in Step 2 using the initial conditions calculated in Step 1 using an adequate method until reaching the desired final simulation time. Optionally, calculate the moments using Equation (20).
4. If needed, reconstruct the distribution function.

The above procedure can be applied to solve any continuous kinetic model in which the reactants and products are represented by only one distribution function. It can be extended for more than one family of compounds, as done by Becker et al.[37] for FPQM.

However, the application of the Step 2 to nonlinear kinetic models generates a system of differential equations that depends

on the distribution function evaluated at the quadrature points. This requires the reconstruction of the distribution by an accurate method, preferably one embedded in other QBMM, as the Modified Sectional DQMoM[41] or the extend quadrature method of moments (EQMoM).[8]

Since the focus of this work was to analyze the applicability of the adaptive characterization method for reactive continuous mixtures and to compare its performance with the method commonly employed to solve these problems (FPQM), the above procedure was applied for three test cases that were modeling with first-order kinetic and only one distribution function. For the first two test cases, analytical solutions do exist and allow us to verify the model accuracy. The third test case has no analytical solution and the DQMoGeM results were compared to FPQM results and to available experimental data. These test cases as well as the corresponding derivation of the DQMoGeM system of differential equations (Step 2) are described in the following sections.

4.1 | Test case 1—Distinct distributions for reactants and products

According to McCoy and Wang,[42] it is not only possible but sometimes necessary to distinguish the distributions of the reactants and products.

Assume the following pseudo-first order irreversible hydrogenation of the reactant family A in isothermal conditions to given the product family B:

$$A(I) + H_2 \overset{k(I)}{\rightarrow} B(I) \tag{23}$$

The rate equations for the consumption of reactant A and formation of product B can be expressed in terms of their molar concentration distribution, f_C^A and f_C^B, respectively (see Equation 2):

$$\frac{\partial f_C^A(I,t)}{\partial t} = -k(I) f_C^A(I,t) \tag{24}$$

$$\frac{\partial f_C^B(I',t)}{\partial t} = k(I) f_C^A(I,t) \tag{25}$$

Assuming I to be the molar mass of the reactant A and I' the molar mass of the product B, the reaction stoichiometry and the molar mass of H_2 allows us to write:

$$I' = I + 2 \tag{26}$$

Following McCoy and Wang,[42] the sum of Equations (24) and (25) gives:

$$\frac{\partial f_C^B(I',t)}{\partial t} = -\frac{\partial f_C^A(I,t)}{\partial t} \tag{27}$$

and, therefore, $f_C^B(I',t)$ is easily obtained from $f^A(I,\ t)$ by integrating Equation (27):

$$f_C^B(I',t) = f_C^A(I,0) - f_C^A(I,t) \tag{28}$$

But $f_C^A(I,t)$ can be analytically determined by solving Equation (24), being given by:

$$f_C^A(I,t) = f_C^A(I,0)\exp(-k(I)t) \tag{29}$$

Thus, for a given initial distribution and a model for $k(I)$, we can obtain the concentration distributions for A and B families along the time. Here we assumed a truncated gamma distribution for $f_C^A(I,0)$, given by:

$$f_C^A(I,0) = d\frac{(I-I_{min})^{a-1}}{b^a\Gamma(a)}\exp\left[-\frac{I-I_{min}}{b}\right],\quad I_{min} \le I \le I_{max} \tag{30}$$

where d is a scaling factor that is determined by:

$$d = \int_{I_{min}}^{I_{max}} f_C^A(I,0)dI = C^A(0), \tag{31}$$

and a power law model for k, given by:

$$k(I) = \sigma I^{\beta} \tag{32}$$

Since the parameter β is the most influential for the reactant conversion, this test case was solved for three different values of β (0.1, 1.0 and 2.0), keeping σ = 0.5 and using the same initial distribution given by Equation (30) with I_{min} = 44, a = 2.1, b = 26.7, and I_{max} = 250. The final time instant was conveniently chosen accordingly to the β value in order to achieve a relevant reactant conversion. Thus, the final simulation times were 1.0, 0.1, and 0.001 for β values equal to 0.1, 1.0, and 2.0, respectively.

The derivation of the DQMoGeM differential equations (Step 2) started by replacing the $f_C^A(I,t)$ in Equation (24) by its discrete form (Equation 16) and expanding the derivatives to obtain:

$$\begin{aligned}\sum_{i=1}^{N}\frac{d\omega_i^A(t)}{dt}\delta\left(I-I_i^A(t)\right) - \sum_{i=1}^{N}\omega_i^A(t)\delta'\left(I-I_i^A(t)\right)\frac{dI_i^A(t)}{dt} \\ = -k(I)\sum_{i=1}^{N}\omega_i^A(t)\delta\left(I-I_i^A(t)\right)\end{aligned} \tag{33}$$

Then, the generalized moment operators, Equation (21), are applied to Equation (33) and the filtering properties of the Dirac delta function, Equation (22), are used to obtain the system of differential equations for the weights and abscissas that determine the moments of the family A distribution:

$$\sum_{i=1}^{N}\frac{d\omega_i^A(t)}{dt}P_j\left(I_i^A(t)\right) + \sum_{i=1}^{N}\omega_i^A(t)\frac{dI_i^A(t)}{dt}P_j'\left(I_i^A(t)\right) = -\sum_{i=1}^{N}\omega_i^A(t)k\left(I_i^A(t)\right)P_j\left(I_i^A(t)\right) \tag{34}$$

4.2 | Test case 2—Pyrolysis of coal tar in a batch reactor

This test case corresponds to the first case analyzed by Mccoy[43] using the fragmentation model, Equation (4), to describe the evolution of the molar mass distribution of a coal during a thermal cracking process in a batch reactor. It assumes binary fragmentation, $\nu(l') = 2$, totally random breakage, $\Omega(l, l') = 1/l'$ and equal reactivity for all reactants, that is, $k_c(l)$ does not depend on l.[42] Thus, Equation (4) can be rewritten in the following form:

$$\frac{\partial f_C(l,t)}{\partial t} = -k_c f_C(l,t) + 2k_c \int_l^{l_{max}} \frac{1}{l'} f_C(l',t)dl' \tag{35}$$

where l_{max} is chosen to be large enough in order to $f_C(l, t) = 0$ for $l > l_{max}$.

Since the distributed variable, l, was assumed to be the molar mass, the zeroth and first-order moments of the f_C distribution are the total molar and mass concentrations. The latter must remain constant along the time for a batch reactor.

Mccoy[43] considered the same initial gamma distribution reported by Chen et al.[44] with parameters obtained from available experimental data. However, Chen et al.[44] neglected the tail of the distribution, $l > 1{,}125$, reasoning that it was responsible for less than 5% of the total initial concentration.

Here we used the truncated gamma distribution (see Equation 30) with the parameters values reported by Chen et al.[44] ($l_{min} = 125$, $a = 1.58$, $b = 192$), but using $l_{max} = 1{,}200$ in order to better compare to Mccoy[43] results. We used the same value of the kinetic rate ($k_c = 0.01838$) applied for the first test case analyzed by Mccoy,[43] which corresponds to the result from the Arrhenius equation, proposed by Chen et al.[44] for the temperature of 660°C.

This case generates an uncoupled system of moment equations than can be solved analytically, which allow easily comparison with numerical results obtained by using the DQMoGeM and FPQM.

In the DQMoGeM Step 2, the distribution $f_C(l, t)$ is replaced by its discrete form (Equation 16) to obtain:

$$\begin{aligned}&\sum_{i=1}^{N} \frac{d\omega_i(t)}{dt}\delta(l-l_i(t)) - \sum_{i=1}^{N}\omega_i(t)\delta'(l-l_i(t))\frac{dl_i(t)}{dt} \\ &= -k_c\sum_{i=1}^{N}\omega_i(t)\delta(l-l_i(t)) + 2k_c\sum_{i=1}^{N}\int_l^{\infty}\frac{1}{l'}\omega_i(t)\delta(l'-l'_i(t))dl'\end{aligned} \tag{36}$$

Then, the generalized moment operators, Equation (21), is applied to Equation (36) and the filtering properties of the Dirac delta function, Equation (22), are used to obtain the following system of differential equations:

$$\begin{aligned}&\sum_{i=1}^{N}\frac{d\omega_i(t)}{dt}P_j(l_i(t)) + \sum_{i=1}^{N}\omega_i(t)\frac{dl_i(t)}{dt}P_j'(l_i(t)) \\ &= -k_c\sum_{i=1}^{N}\omega_i(t)P_j(l_i(t)) + 2k_c\sum_{i=1}^{N}\frac{\omega_i(t)G_j(l_i)}{l_i(t)}\end{aligned} \tag{37}$$

where

$$G_j(l_i) = \int_0^{l_i} P_j(l)dl \tag{38}$$

which can be analytically calculated.

4.3 | Test case 3—Hydrocracking of heavy oils

This case was originally presented by Elizalde and Ancheyta.[34] They made a review of the kinetic model developed by Laxminarasimhan et al.,[15] showing in detail the mathematical formulation of the FPQM and how it is applied to hydrocracking problems assuming first-order reaction for all pseudo-components.

Elizalde and Ancheyta[34] estimated the parameters of the model (α, k_{max}, a_0, a_1, and ψ) using their own experimental data, collected from a bench-scale plant during the moderate hydrocracking of Maya crude oil. They used the Levenberg–Marquardt optimization algorithm to fit the parameters to the resulting data from the application of the FPQM.

In this work, the experimental data from Elizalde and Ancheyta[34] and their adjusted values for the model parameters ($\alpha = 0.245$, $k_{max} = 0.537h^{-1}$, $a_0 = 1.396$, $a_1 = 22.0$, and $\psi = 4.46 \times 10^{-5}$) were used to compare the numerical solutions from both FPQM and DQMoGeM.

Since the DQMoGeM is based on the evolution of the distribution moments, Equation (10) was first converted back to its form in terms of the mass fraction distribution, that is, using Equations (11), (12) and (14), Equation (10) can be rewritten as:

$$\frac{df_w(\theta,t)}{dt} = -k_{max}\theta^{(1/\alpha)}f_w(\theta,t) + n\int_\theta^1 p(\theta,\theta')k_{max}\theta'^{(1/\alpha)}f_w(\theta',t)d\theta' \tag{39}$$

where, from the $p(k, k')$ definition,[15] we can write:

$$p(\theta,\theta') = \frac{1}{S_0(\theta')\sqrt{2\pi}}\left\{\exp-\left[\frac{(\theta/\theta')^{(a_0/\alpha)}-0.5}{a_1}\right]^2 - \mathcal{A} + \mathcal{B}(\theta,\theta')\right\} \tag{40}$$

$$\mathcal{A} = \exp\left[-(0.5/a_1)^2\right] \tag{41}$$

$$\mathcal{B}(\theta,\theta') = \psi\left[1-\left(\frac{\theta}{\theta'}\right)^{(1/\alpha)}\right] \tag{42}$$

$$S_0(\theta') = n\int_0^{\theta'}\frac{1}{\sqrt{2\pi}}\left\{\exp-\left[\frac{(\theta/\theta')^{(a_0/\alpha)}-0.5}{a_1}\right]^2 - \mathcal{A} + \mathcal{B}(\theta,\theta')\right\}d\theta \tag{43}$$

After replacing the distribution $f_w(\theta, t)$ by its discrete form, Equation (39) can be converted to:

$$\begin{aligned}&\frac{\partial}{\partial t}\left[\sum_{i=1}^{N}\omega_i(t)\delta(\theta-\theta_i(t))\right] = -k_{max}\sum_{i=1}^{N}\omega_i(t)\theta^{(1/\alpha)}\delta(\theta-\theta_i(t)) \\ &+ nk_{max}\sum_{i=1}^{N}\omega_i(t)\int_\theta^1 p(\theta,\theta')\theta'^{(1/\alpha)}\delta(\theta'-\theta'_i(t))d\theta'\end{aligned} \tag{44}$$

Then, the application of the generalized moment operators, Equation (21), and the filtering properties of the Dirac delta functions, Equation (22), transforms Equation (44) into:

$$\begin{aligned}\sum_{i=1}^{N}\frac{d\omega_i(t)}{dt}P_j(\theta_i(t))-\sum_{i=1}^{N}\omega_i(t)\frac{d\theta_i(t)}{dt}P_j'(\theta_i(t))\\ =-k_{max}\sum_{i=1}^{N}\omega_i(t)\theta_i(t)^{(1/\alpha)}P_j(\theta_i(t))\\ +nk_{max}\sum_{i=1}^{N}\omega_i(t)\theta_i(t)^{(1/\alpha)}H_j(\theta_i(t))\end{aligned} \tag{45}$$

where

$$H_j(\theta')=\int_0^{\theta'}P_j(\theta)p(\theta,\theta')d\theta \tag{46}$$

It is important to highlight that there is no n dependence in the last term of Equation (45). This can be seen by the fact that $p(\theta, \theta')$, Equation (40), is inversely proportional to $S_0(\theta')$, Equation (43), which in turn is proportional to n. Therefore, the n factor in the last term of Equation (45) cancels out.

For this case, the DQMoGeM results were used to reconstruct the distribution using the Fourier series,[1] which can be directly compared to our FPQM results. It should be noted that our FPQM results are very similar to those reported by Elizalde and Ancheyta.[34]

5 | NUMERICAL PROCEDURE

The numerical procedures described in this section were implemented in routines written mainly in the *C#* language, but using some routines written in C and FORTRAN: the Differential-Algebraic System Solver in C (DASSLC),[45] ORTHPOL,[46] and AUTOQUAD[47] packages. All computations were performed using double precision (16 significant digits) on a laptop with an Intel Quadricore i7 processor at 2.8 GHz and 8 Gb of RAM.

The three test cases described in the previous section involve distributions in finite domains. Therefore, the DQMoGeM using the moments based on Legendre polynomials was chosen for their solution.

The second and third test cases were solved using both DQMoGeM and FPQM. For performance comparison, care was taken to use the same numerical procedures for the similar tasks in both methods and to employ the same criteria for verifying their accuracy.

5.1 | Calculation of the moments of the initial distribution

Using Equation (18), the initial values of the Legendre generalized moments were calculated by:

$$\mu_j(0)=\int_{l_{min}}^{l_{max}}\ell_j(l)f(l,0)dl,\quad j=0,\ldots,2N-1 \tag{47}$$

Since it was not possible to obtain analytical expressions for these moments for the test cases, the integrations in Equation (47) were numerically computed using the adaptive domain-splitting scheme using the interlaced set of Gauss–Kronrod quadratures implemented in the AUTOQUAD routine.[47] A relative accuracy of 10^{-12} was requested for all moments.

5.2 | Calculation of the quadrature rule

The modified Chebyshev algorithm was chosen to obtain the quadrature weights and abscissas from the moments of the distribution. The computation was performed using the subroutines *dcheb* and *dgauss* of the ORTHOPOL package.[48]

5.3 | Solution of the system of differential equations

The solution of the system of differential equations was performed using the DASSLC package.[45] This package uses the backward differentiation formula (BDF) of variable order and adaptive time step to guarantee a desired accuracy. For all variables in all test cases, we employed values for the relative and absolute tolerances equal to 10^{-8} and 10^{-10}, respectively.

5.4 | Reconstruction of the distribution function

The reconstruction of the distribution function was performed using the simple functional reconstruction given by Lage.[1] In this Fourier series expansion method, the Legendre polynomials were calculated from the three-term recurrence relation of orthogonal polynomials, whose coefficients were calculated using the *drecur* subroutine of the ORTHOPOL package.[48]

5.5 | Convergence analysis

Since the analytical solution is known for the first test case, the following equation was used to evaluate the time-average relative error of each moment:

$$\varepsilon_j=\frac{1}{nt}\sum_{s=1}^{nt}\left|\frac{\mu_j^a(t_s)-\mu_j(t_s)}{\mu_j^a(t_s)}\right| \tag{48}$$

where μ_j^a are the moments calculated from the analytical solution at each time t_s, using the same procedure described in section 5.1, and nt is the number of time steps.

For the first test case, the number of quadrature points (nodes) was progressively increased until the convergence criterion, which was defined as $\varepsilon_j < 10^{-6}$ for all calculated moments, was reached.

For the second test case, Equation (48) was also used to evaluate the error. However, the convergence criteria was adopted only for the first-order moment, that is, $\varepsilon_1 < 0.01$. As discussed elsewhere, the first-order moment is the total mass concentration and

must remain constant along the time for a batch reactor, that is, $\mu_1(t_s)\ /\mu_1^q(0) = 1, \forall t_s$.

For the third test case, two convergence criteria were used for both the FPQM and DQMoGeM. The first was given by $\varepsilon_0 < 5 \times 10^{-4}$ using Equation (48). The second criterion was based in the average of the squares of the errors in the cumulative mass distribution, F_w, given by:

$$\zeta = \frac{1}{n}\sum_{s=1}^{n}\left(F_{w,s}^{e} - F_{w,s}\right)^2, \quad F_{w,s} = \frac{\sum_{i=1}^{s} W_i}{\sum_{i=1}^{n} W_i} \tag{49}$$

where the superscript e was used to represent the experimental values. The second convergence criterion was $\zeta < 1.5 \times 10^{-4}$. The number of quadrature points, N, and the number of lumps, n, were

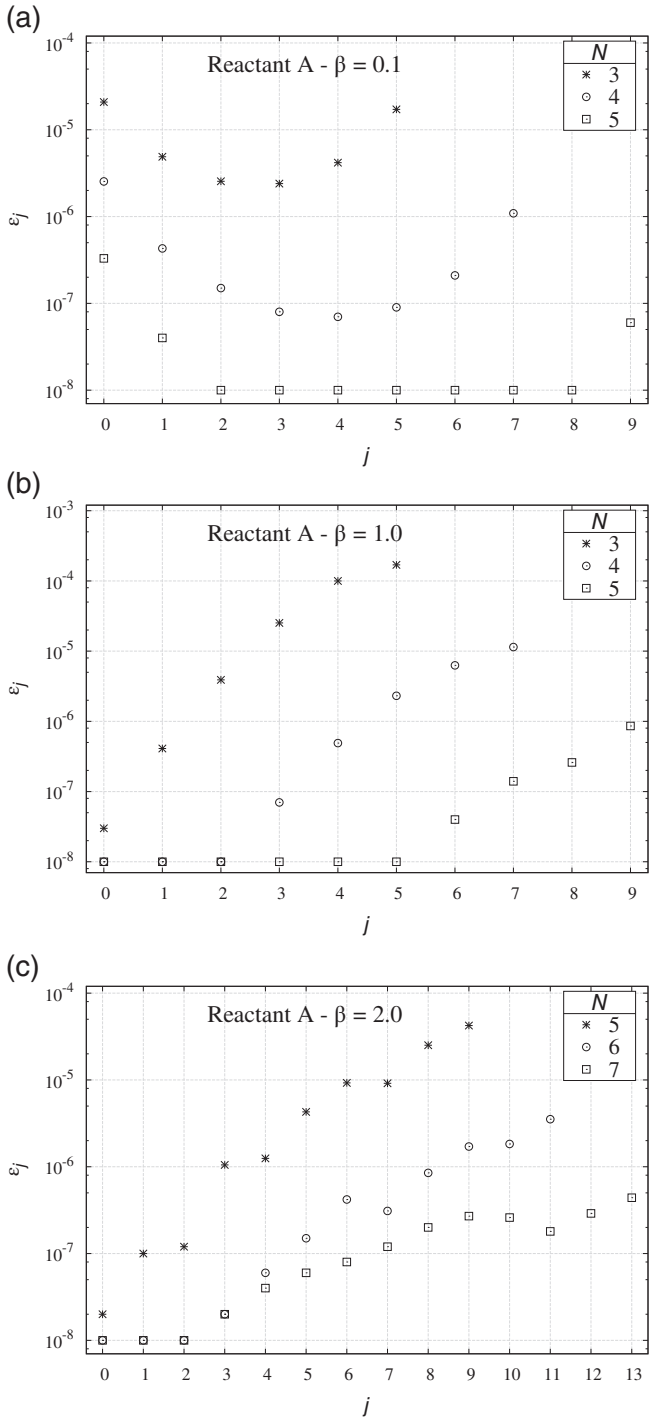

FIGURE 1 Time-average relative error for all solved moments of the reactant A concentration distribution, $\mu_j, j = 0, \ldots, 2N-1$, for test case 1 with (a) $\beta = 0.1$, (b) $\beta = 1.0$, and (c) $\beta = 2.0$

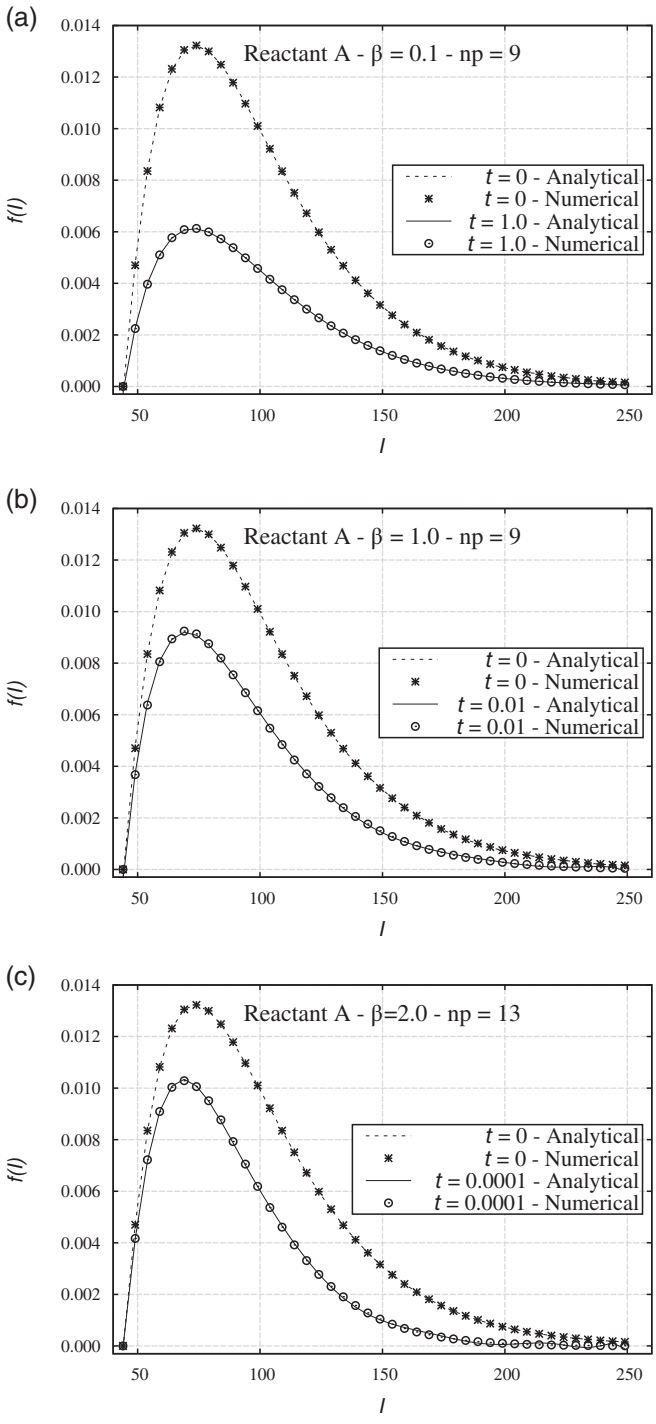

FIGURE 2 Reconstructed concentration distribution of the reactant A for test case 1 with (a) $\beta = 0.1$ ($N = 5$ and $np = 9$), (b) $\beta = 1.0$ ($N = 5$ and $np = 9$), and (c) $\beta = 2.0$ ($N = 7$ and $np = 13$)

chosen to be the smallest ones that give results that satisfied both criteria.

Although the code was not fully optimized, the third case was also used to compare the performance of FPQM and DQMoGeM, by using the average CPU times of 3 runs.

6 | RESULTS AND DISCUSSION

6.1 | Test case 1—Distinct distributions for reactants and products

Figure 1a–c presents the time-averaged relative errors for all moments solved by DQMoGeM, ε_j, j = 0, …, 2 N − 1, of the reactant A concentration distribution for the simulations with β = 0.1, 1.0, and 2.0, respectively. It can be seen that the desirable accuracy of 10^{-6} was reached with N = 5 for β = 0.1 and 1.0, and with N = 7 for the case with more abrupt variation in the reactant concentration (β = 2.0).

It can be seen that the numerical e analytical results agree very well for the simulations with the three β values. However, the abscissas were almost constant during the simulation and, therefore, it was not possible to observe the DQMoGeM adaptability for this case during the solution.

Figure 2a–c shows the reconstructed distributions obtained using np = 2 N − 1 for the simulations with β = 0.1, 1.0, and 2.0, respectively. They show that the Lage[1] reconstruction method was adequate to represent the distributions for these cases.

6.2 | Test case 2—Pyrolysis of coal tar in a batch reactor

Figure 3a,b shows, respectively, the evolution of the zeroth and first-order moments of the concentration distribution normalized by their analytical values, $\mu_j/\mu_j^a, j = 0,1$, obtained using the FPQM with several numbers of lumps, n. It can be seen that the FPQM method needs at least 75 lumps to achieve the desirable accuracy ($\varepsilon_1 < 0.01$). On the other hand, the DQMoGeM using $N \geq 1$ gave results (not shown) for which $\mu_j/\mu_j^a - 1 \tilde{} 10^{-15}, j = 0,1$, that is, their errors were almost in the order of the machine precision, whatever the value of N.

Figure 4a shows the evolution of the approximated distribution calculated using the FPQM with n lumps whereas Figure 4b shows the evolution for the reconstructed distribution obtained from the DQMoGeM

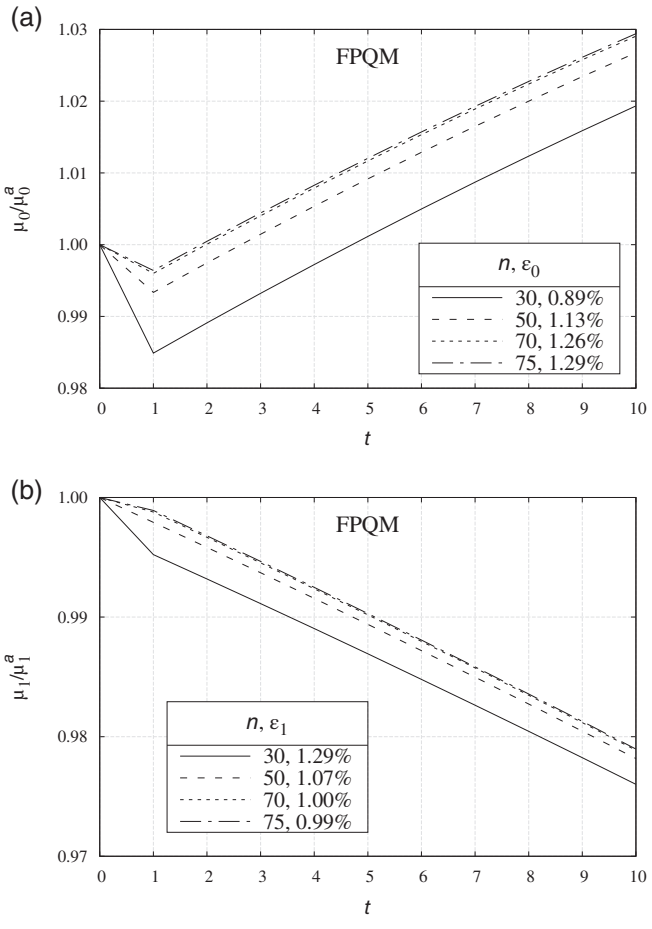

FIGURE 3 Time evolution of the two first moments of the concentration distribution (total molar concentration and total mass) for the solutions of test case 2 obtained using the FPQM, (a) μ_0/μ_0^a and (b) μ_1/μ_1^a

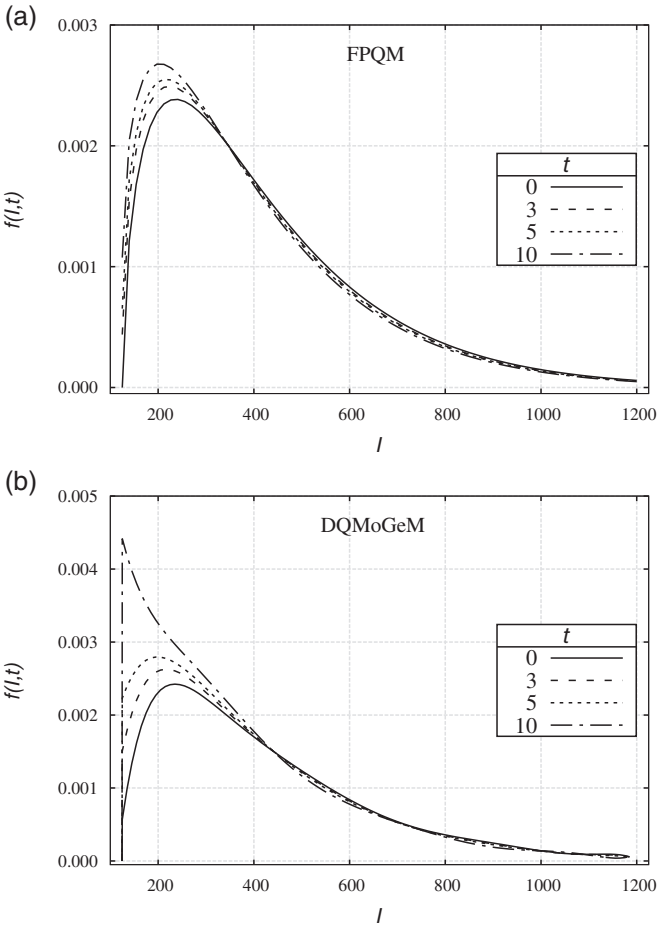

FIGURE 4 Time evolution of the reconstructed distributions for the solutions of test case 2 obtained by the (a) FPQM (n = 75) and (b) DQMoGeM (N = 5 and np = 9)

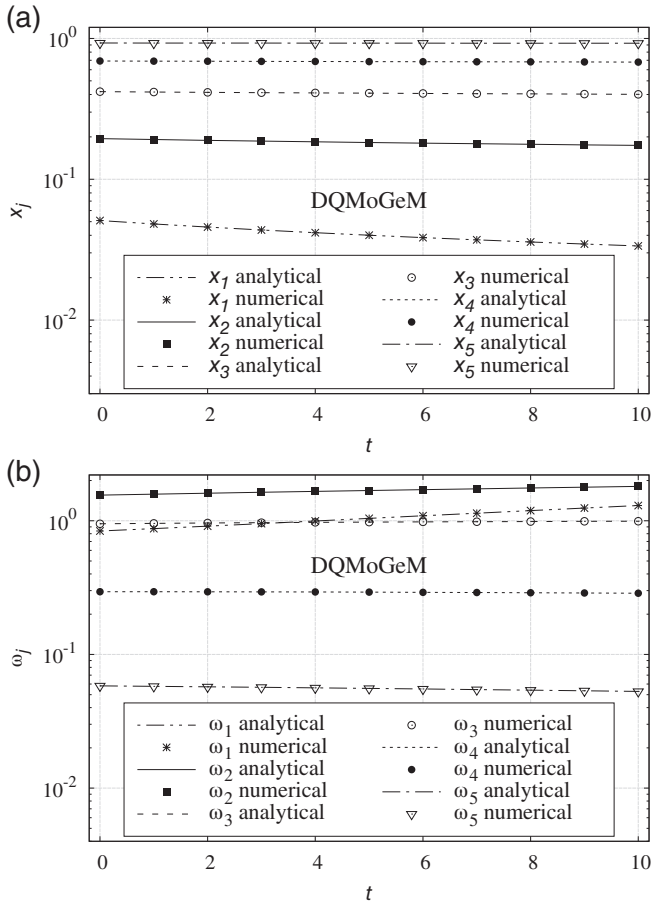

FIGURE 5 Time evolution of the (a) normalized abscissas, x_j, and (b) weights for the DQMoGeM solution with $N = 5$ for test case 2

results using the Fourier series.[1] In this case, the number of quadrature points N was progressively increased up to the reconstructed distribution using $np = 2N - 1$ showed no further significant changes.

The shapes of the resulting distributions shown in Figure 4b are very similar to those originally obtained by Mccoy[43] by fitting the data to gamma distributions. On the other hand, the FPQM was not able to capture sudden variations like the concentration peak at the lower bound of the domain for $t = 10$, which led to a significant error.

The time evolution of the abscissas and the weights are show in Figures 5a,b, respectively. It is clear that the abscissas change along the time for this case, demonstrating the adaptive characteristic of the DQMoGeM.

6.3 | Test case 3—Hydrocracking of heavy oils

In order to directly compare our FPQM results and the experimental data for the cumulative mass fraction distribution given by Elizalde and Ancheyta,[34] the Fourier series[1] was used to reconstruct the distribution from the DQMoGeM results, from which the cumulative distribution was calculated.

Figure 6 shows the comparison among the experimental data and the FPQM and DQMoGeM results obtained in this work. The agreement with the experimental data is really good for DQMoGeM and even

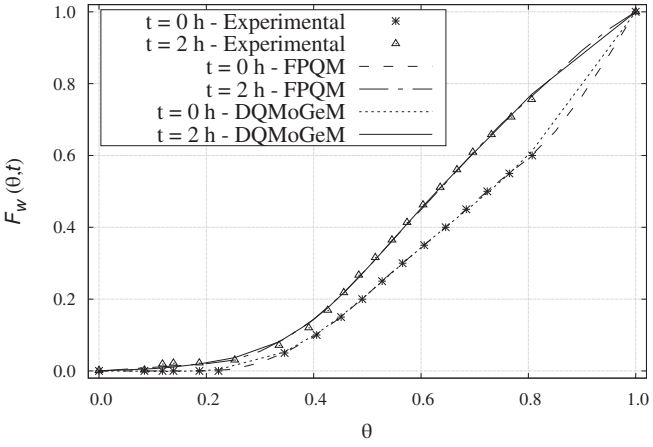

FIGURE 6 Comparison of the results for the cumulative distribution of mass fraction for test case 3 obtained using FPQM and DQMoGeM ($N = 5$ and $np = 9$) with the experimental data

better for FPQM. However, it is important to highlight that the FPQM advantage over DQMoGeM was already expected, because the model parameters were adjusted using the results of FPQM simulations.

As discussed by Elizalde and Ancheyta,[34] the FPQM needed at least 150 lumps to achieve the desirable accuracy in the mass balance ($\varepsilon_1 < 5 \times 10^{-4}$), which was the most restrictive criterion for the FPQM. The second criterion, that is, $\zeta < 1.5 \times 10^{-4}$ (see Equation 49) was more easily satisfied.

On the other hand, the Appendix shows that the DQMoGeM always satisfies the mass balance for all N values. However, it was necessary to progressively increase the number of quadrature points up to $N = 5$ in order to satisfy the second criterion, $\zeta < 1.5 \times 10^{-4}$.

The CPU time for the FPQM simulation ($n = 150$) was about 11 min, whereas the DQMoGeM simulation ($N = 5$) took just 5 s, clearly showing that the DQMoGeM is much faster than the FPQM. This more than 100-fold increase in the model solution speed allows a much faster model parameter estimation and the easier exploration of new model functions for p and θ.

7 | CONCLUSIONS

This work shows that the proposed methodology can be used to solve kinetic models of continuous mixtures. Due its larger accuracy, speedups larger than 100 were obtained for the model solution when it was compared to the solution method proposed by Laxminarasimhan et al.[15] (FPQM).

The DQMoGeM was able to carry out simulations that are extremely accurate in terms of the mass balance for any number of quadrature points, whereas the FPQM required more than 40 lumps to achieve an acceptable accuracy for the mass conservation in the analyzed hydrocracking problems.

The reconstruction by Fourier series[1] proved to be sufficiently accurate to analyze the DQMoGeM results when the distribution is needed.

ACKNOWLEDGMENTS

Paulo L. C. Lage acknowledges the financial support from CNPq, grants nos. 456905/2014-6 and 305265/2015-6, and from FAPERJ, grant no. E-26/111.361/2010. This study was financed in part by the Coordenação de Aperfeiçoamento de Pessoal de Nível Superior—Brasil (CAPES)—Finance Code 001.

NOMENCLATURE

a	parameter in the gamma distribution function
a_0	parameter a_0 of yield distribution function
a_1	parameter a_1 of yield distribution function
$\mathcal{A}$	function defined by Equation (41)
b	parameter in the gamma distribution function
$\mathcal{B}$	function defined by Equation (42)
b_f	breakage frequency
C	molar concentration
c	molar concentration of individual component in distribution
D	distribution of the number of lumps
d	scaling factor in Equation (30)
F	cumulative distribution
f	distribution function
G	function defined by Equation (38)
H	function defined by Equation (46)
I	generic distribution variable (e.g., molar mass) or quadrature abscissa
k	kinetic rate or reactivity
k_c	constant kinetic rate
ℓ	Legendre polynomial
N	number of quadrature points (discretized pseudo-components)
n	number of lumps
N_{Av}	Avogadro number
np	number of terms of the Fourier series
nt	total number of time steps
P	polynomial
p	yield distribution function
pn	total number of particles per unit volume
q	reaction order
S_0	parameter S_0 of yield distribution function
t	time
TBP	true boiling point temperature
w	mass or mass fraction distribution
$\mathcal{W}$	weight function in polynomial orthogonality property
W_i	mass of lump i
x_j	normalized quadrature abscissa, $x_j = (I_j - I_{min})/(I_{max} - I_{min})$

GREEK LETTERS

α	parameter in the mixture reactivity model
β	parameter in Equation (32)
δ	dirac delta function
ε	time-averaged relative error
ζ	mean square deviation of the cumulative mass distribution
Γ	Gamma function
θ	normalized TBP
κ	overall rate function
μ	generalized moment
ν	the average number of particles formed from the breakup of a single particle of state I'
ω	quadrature weight
Ω	probability distribution for the fragmentation
σ	parameter in Equation (32)
ψ	parameter in yield distribution function

SUBSCRIPTS

C	molar concentration
max	maximum value
min	minimum value
w	mass

SUPERSCRIPTS

A A FAMILY OF MIXTURE COMPONENTS
a analytical
B B family of mixture components
e experimental

NOTATION

BDF	backward differentiation formula
DASSLC	Differential-Algebraic System Solver in C
DQMoGeM	direct quadrature method of generalized moments
DQMoM	direct quadrature method of moments
EQMoM	extend quadrature method of moments
FPQM	fixed point quadrature method
LQMDA	Long Quotient-Modified Difference Algorithm
MoM	method of moments
PBE	population balance equation
QBMM	quadrature-based moment methods
QMoM	quadrature method of moments

ORCID

Paulo L. C. Lage https://orcid.org/0000-0002-0396-5508

REFERENCES

1. Lage PLC. The quadrature method of moments for continuous thermodynamics. *Comput Chem Eng*. 2007;31(7):782-799.
2. Okino MS, Mavrovouniotis ML. Simplification of mathematical models of chemical reaction systems. *Chem Rev*. 1998;98(2):391-408.
3. Ramkrishna D. *Population Balances—Theory and Applications to Particulate Systems in Engineering*. San Diego: Academic Press; 2000.
4. McGraw R. Description of aerosol dynamics by the quadrature method of moments. *Aerosol Sci Tech*. 1997;27(2):255-265.
5. Marchisio DL, Fox RO. Solution of population balance equations using the direct quadrature method of moments. *J Aerosol Sci*. 2005;36(1):43-73.

6. Grosch R, Briesen H, Marquardt W, Wulkow M. Generalization and numerical investigation of QMOM. *AIChE J*. 2007;53(1):207-227.
7. Lage PLC. On the representation of QMOM as a weighted-residual method—the dual-quadrature method of generalized moments. *Comput Chem Eng*. 2011;35(11):2186-2203.
8. Yuan C, Laurent F, Fox RO. An extended quadrature method of moments for population balance equations. *J Aerosol Sci*. 2012;51:1-23.
9. Laurent C, Lavergne G, Villedieu P. Continuous thermodynamics for droplet vaporization: comparison between gamma-PDF model and QMoM. *CR Mécanique*. 2009;337(6):449-457.
10. Laurent C, Lavergne G, Villedieu P. Quadrature method of moments for modeling multi-component spray vaporization. *Int J Multiph Flow*. 2010;36(1):51-59.
11. Rodrigues RC, Ahón VRR, Lage PLC. An adaptive characterization scheme for the simulation of multistage separation of continuous mixtures using the quadrature method of moments. *Fluid Phase Equilib*. 2012;318(suppl C):1-12.
12. Petitfrere M, Nichita DV, Montel F. Multiphase equilibrium calculations using the semi-continuous thermodynamics of hydrocarbon mixtures. *Fluid Phase Equilib*. 2014;362(suppl C):365-378.
13. Jatobá LFC, Lage PLC, Silva LFLR. Simulation of the compressible flow with mass transfer of semi-continuous mixtures using the direct quadrature method of moments. *Comput Chem Eng*. 2014;64:153-166.
14. Santos FP, Lage PLC, Fontes CE. Numerical aspects of direct quadrature-based moment methods for solving the population balance equation. *Braz J Chem Eng*. 2013;30(3):643-656.
15. Laxminarasimhan CS, Verma RP, Ramachandran PA. Continuous lumping model for simulation of hydrocracking. *AIChE J*. 1996;42(9):2645-2653.
16. De Donder T. *L'affinité. No. 2 in L'affinité*. Paris: Gauthier Villars; 1931.
17. Gal-Or B, Cullinan HT, Galli R. New thermodynamic-transport theory for systems with continuous component density distributions. *Chem Eng Sci*. 1975;30(9):1085-1092.
18. Briano JG, Glandt ED. Molecular thermodynamics of continuous mixtures. *Fluid Phase Equilib*. 1983;14:91-102.
19. Cotterman RL, Prausnitz JM. Continuous thermodynamics for phase-equilibrium calculations in chemical process design. In: Astarita G, Sandler SI, eds. *Kinetic and Thermodynamic Lumping of Multicomponent Mixtures*. Amsterdam: Elsevier; 1991:229-275.
20. Amhammed MA. Applications of Lumping Kinetics Methodology to Complex Reactive Mixtures [dissertation]. Heriot-Watt University; 2013.
21. Aris R, Gavalas GR. On the theory of reactions in continuous mixtures. *Philos Trans R Soc Lond A*. 1966;260(1112):351-393.
22. Ho TC, Aris R. On apparent second-order kinetics. *AIChE J*. 1987;33(6):1050-1051.
23. Astarita G, Ocone R. Lumping nonlinear kinetics. *AIChE J*. 1988;34(8):1299-1309.
24. Aris R. Reactions in continuous mixtures. *AIChE J*. 1989;35(4):539-548.
25. Chou MY, Ho TC. Continuum theory for lumping nonlinear reactions. *AIChE J*. 1988;34(9):1519-1527.
26. Saito O. On the effect of high energy radiation to polymers: I. Cross-linking and degradation. *J Physical Soc Japan*. 1958;13(2):198-206.
27. Ziff RM, McGrady ED. The kinetics of cluster fragmentation and depolymerisation. *J Phys A Math Gen*. 1985;18(15):3027-3037.
28. Browarzik D, Kehlen H. Hydrocracking process of n-alkanes by continuous kinetics. *Chem Eng Sci*. 1994;49(6):923-926.
29. Peixoto FC, Medeiros JL. Reactions in multiindexed continuous mixtures: catalytic cracking of petroleum fractions. *AIChE J*. 2001;47(4):935-947.
30. Khorasheh F, Chan EC, Gray MR. Development of a continuous kinetic model for catalytic hydrodesulfurization of bitumen. *Pet Coal*. 2005;47:39.
31. Ashuri E, Khorasheh F, Gray MR. Development of a continuous kinetic model for catalytic hydrodenitrogenation of bitumen. *Scientia Iranica*. 2007;14(2):152-160.
32. Elizalde I, Rodríguez MA, Ancheyta J. Application of continuous kinetic lumping modeling to moderate hydrocracking of heavy oil. *Appl Catal Gen*. 2009;365(2):237-242.
33. Shadbahr J, Khosravani L, Khorasheh F. Development of a continuous kinetic model for visbreaking reactions. *Scientia Iranica*. 2011;18(3):465-469.
34. Elizalde I, Ancheyta J. On the detailed solution and application of the continuous kinetic lumping modeling to hydrocracking of heavy oils. *Fuel*. 2011;90(12):3542-3550.
35. Adam M, Calemma V, Galimberti F, Gambaro C, Heiszwolf J, Ocone R. Continuum lumping kinetics of complex reactive systems. *Chem Eng Sci*. 2012;76:154-164.
36. Ghane A, Khorasheh F. Development of a continuous kinetic model for prediction of coke formation in hydroconversion of marlim crude oil in a slurry-phase reactor. *Petrol Coal*. 2014;56(3):259-266.
37. Becker PJ, Celse B, Guillaume D, Dulot H, Costa V. Hydrotreatment modeling for a variety of VGO feedstocks: a continuous lumping approach. *Fuel*. 2015;139:133-143.
38. Elizalde I, Trejo F, Muñoz JAD, Torres P, Ancheyta J. Dynamic modeling and simulation of a bench-scale reactor for the hydrocracking of heavy oil by using the continuous kinetic lumping approach. *React Kinet Mech Catal*. 2016;118(1):299-311.
39. Hulburt HM, Katz S. Some problems in particle technology. *Chem Eng Sci*. 1964;19(8):555-574.
40. Gautschi W. Construction of Gauss–Christoffel quadrature formulas. *Math Comput*. 1968;22(102):251-270.
41. Massot M, Laurent F, Kah D, De Chaisemartin S. A robust moment method for evaluation of the disappearance rate of evaporating sprays. *SIAM J Appl Math*. 2010;70(8):3203-3234.
42. McCoy BJ, Wang M. Continuous-mixture fragmentation kinetics: particle size reduction and molecular cracking. *Chem Eng Sci*. 1994;49(22):3773-3785.
43. Mccoy BJ. Continuous kinetics of cracking reactions: thermolysis and pyrolysis. *Chem Eng Sci*. 1996;51(11):2903-2908.
44. Chen WY, Zhang ZP, Shen BC, Fan LT. Stochastic modeling of tar molecular weight distribution during coal pyrolysis. *Chem Eng Sci*. 1994;49(22):3687-3698.
45. Secchi AR. DASSLC user's manual—v3.2 (Diferential-Algebraic System Solver in C); 2007. https://www.ufrgs.br/dequi-app/enqlib/numeric/numeric.html. Accessed: May 01, 2017.
46. Gautschi W. *Orthogonal Polynomials—Computation and Approximation*. Oxford: Oxford University Press; 2004.
47. Lage PLC, Rangel RH. Total thermal radiation absorption by a single spherical droplet. *J Thermophys Heat Transf*. 1993;7(1):101-109.
48. Gautschi W. Algorithm 726: ORTHPOL—a package of routines for generating orthogonal polynomials and Gauss-type quadrature rules. *ACM Trans Math Softw*. 1994;20(1):21-62.

SUPPORTING INFORMATION

Additional supporting information may be found online in the Supporting Information section at the end of this article.

How to cite this article: Rocha DC, Lage PLC. The solution of continuous kinetic lumping models using the adaptive characterization method. *AIChE J*. 2020;66:e16758. https://doi.org/10.1002/aic.16758